British Journal of Pharmacology

British Journal of Pharmacology (2017) **174** 4396–4408 4396

RESEARCH PAPER

A new negative allosteric modulator, AP14145, for the study of small conductance calcium-activated potassium ($K_{Ca}2$) channels

Correspondence Bo H. Bentzen, Biomedical Institute, University of Copenhagen, Blegdamsvej 3B, DK-2200 Copenhagen, Denmark. E-mail: bobe@sund.ku.dk

Received 10 March 2017; **Revised** 8 September 2017; **Accepted** 13 September 2017

Rafel Simó-Vicens[1,2], Jeppe E Kirchhoff[2], Bernardo Dolce[3], Lea Abildgaard[2], Tobias Speerschneider[2], Ulrik S Sørensen[2], Morten Grunnet[2], Jonas G Diness[2] and Bo H Bentzen[1,2]

[1]Biomedical Institute, University of Copenhagen, Copenhagen, Denmark, [2]Acesion Pharma, Copenhagen, Denmark, and [3]Department of Experimental Pharmacology and Toxicology, University Medical Center Hamburg-Eppendorf, DZHK (German Center for Cardiovascular Research), Partner Site Hamburg/Kiel/Lübeck, Hamburg, Germany

BACKGROUND AND PURPOSE

Small conductance calcium-activated potassium ($K_{Ca}2$) channels represent a promising atrial-selective target for treatment of atrial fibrillation. Here, we establish the mechanism of $K_{Ca}2$ channel inhibition by the new compound AP14145.

EXPERIMENTAL APPROACH

Using site-directed mutagenesis, binding determinants for AP14145 inhibition were explored. AP14145 selectivity and mechanism of action were investigated by patch-clamp recordings of heterologously expressed $K_{Ca}2$ channels. The biological efficacy of AP14145 was assessed by measuring atrial effective refractory period (AERP) prolongation in anaesthetized rats, and a beam walk test was performed in mice to determine acute CNS-related effects of the drug.

KEY RESULTS

AP14145 was found to be an equipotent negative allosteric modulator of $K_{Ca}2.2$ and $K_{Ca}2.3$ channels (IC_{50} = 1.1 ± 0.3 μM). The presence of AP14145 (10 μM) increased the EC_{50} of Ca^{2+} on $K_{Ca}2.3$ channels from 0.36 ± 0.02 to 1.2 ± 0.1 μM. The inhibitory effect strongly depended on two amino acids, S508 and A533 in the channel. AP14145 concentration-dependently prolonged AERP in rats. Moreover, AP14145 (10 $mg \cdot kg^{-1}$) did not trigger any apparent CNS effects in mice.

CONCLUSIONS AND IMPLICATIONS

AP14145 is a negative allosteric modulator of $K_{Ca}2.2$ and $K_{Ca}2.3$ channels that shifted the calcium dependence of channel activation, an effect strongly dependent on two identified amino acids. AP14145 prolonged AERP in rats and did not trigger any acute CNS effects in mice. The understanding of how $K_{Ca}2$ channels are inhibited, at the molecular level, will help further development of drugs targeting $K_{Ca}2$ channels.

Abbreviations

AERP, atrial effective refractory period; AF, atrial fibrillation; $K_{Ca}1.1$, big conductance calcium-activated potassium channel; $K_{Ca}2$, small conductance calcium-activated potassium channel; $K_{Ca}3.1$, intermediate conductance calcium-activated potassium channel; PEG, polyethylene glycol; WT, wild type

DOI:10.1111/bph.14043

Introduction

Small conductance calcium-activated potassium channels (**$K_{Ca}2.1$**, **$K_{Ca}2.2$** and **$K_{Ca}2.3$**) are widely distributed in humans (Chen *et al.*, 2004), where they serve important roles such as contributing to the afterhyperpolarization in neurons (Pedarzani *et al.*, 2005), the endothelium-derived hyperpolarization (Milkau *et al.*, 2010) or the late repolarization phase in cardiomyocytes (Li *et al.*, 2009). These channels are constitutively associated with calmodulin, which binds intracellular calcium and activates $K_{Ca}2$ channels (Adelman, 2016). Ever since the cloning of the channels 20 years ago (Köhler *et al.*, 1996), they have piqued the interest of pharmacologists in different therapeutic areas. Although at the beginning most of the efforts were focused on the CNS and the treatment of neurodegenerative and psychiatric diseases (Lam *et al.*, 2013), the therapeutic potential of $K_{Ca}2$ channels rapidly spread to other areas (Wulff *et al.*, 2007). Currently, one of the most promising therapeutic opportunities for $K_{Ca}2$ channel modulation seems to be in cardiovascular diseases, more specifically in atrial fibrillation (AF).

AF is the most common type of cardiac arrhythmia, and it is considered one of the largest public health problems in developed countries (Zoni-Berisso *et al.*, 2014). The disease is characterized by rapid uncoordinated activation of the atria, resulting in reduced ventricular filling and blood stasis in atria, which predisposes to heart failure and thromboembolic stroke (Nattel, 2002). Unfortunately, current rhythm therapy is only moderately effective and may trigger serious non-cardiac as well as ventricular adverse effects (Waks and Zimetbaum, 2017).

$K_{Ca}2$ channels are considered a promising new target for AF treatment for several reasons. First, the functional role of $K_{Ca}2.2$ and $K_{Ca}2.3$ channels appears to be greater in the atria, than in to the ventricles and that difference may help in avoiding undesired adverse ventricular effects (Diness *et al.*, 2015). Second, $K_{Ca}2$ channel inhibition prolongs the atrial effective refractory period (AERP, Diness *et al.*, 2010), a pharmacological strategy that has successfully been used in the development of other class III antiarrhythmic drugs (Schmitt *et al.*, 2014). Furthermore, common variants of the genes that encode $K_{Ca}2.2$ and $K_{Ca}2.3$ have been associated with AF (Ellinor *et al.*, 2010; Christophersen *et al.*, 2017).

The first described negative allosteric modulator was **NS8593** (Figure 1), a chiral 2-aminobenzimidazole derivative able to inhibit $K_{Ca}2$ channels at nanomolar concentrations with no subtype selectivity (Strøbæk *et al.*, 2006; Sørensen *et al.*, 2008). The negative modulation of NS8593 derives from the compound's ability to increase the EC_{50} of Ca^{2+} for the activation of $K_{Ca}2$ channels and its binding site has been found to be in the inner pore vestibule of the channel (Jenkins *et al.*, 2011).

$K_{Ca}2$ channels are widely expressed in the CNS (Stocker and Pedarzani, 2000), and therefore, one of the challenges encountered during the development of compounds targeting peripheral $K_{Ca}2$ channels is the possibility of adverse effects, mediated by actions in the CNS (Habermann, 1984). It is thus important to develop compounds with reduced blood–brain barrier penetrance in order to avoid possible adverse effects. In this work, we present a novel $K_{Ca}2$ channel negative allosteric modulator, AP14145 (Figure 1), a structurally close analogue of NS8593 designed to inhibit specifically peripheral $K_{Ca}2$ channels by preventing its entry in the CNS. In contrast to NS8593, it does not appear to have any immediate CNS effects when given to rodents and therefore represents a new and improved tool compound for studying $K_{Ca}2$ channel inhibition in rodents *in vivo*.

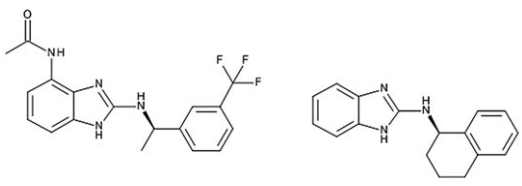

Figure 1
Chemical structures of AP14145 (left) and NS8593 (right).

Methods

Molecular biology

$rK_{Ca}2.3$ wild type (WT) and $rK_{Ca}2.3$ S508T A533V were inserted in pXOON plasmids. The $rK_{Ca}2.3$ NS8593 insensitive mutant was obtained by introducing the double point mutation to the WT $rK_{Ca}2.3$ with the oligonucleotides CCATAG CCAATggtAAGGAACGTGATG for S508T and CATCATGGG TgtaGGCTGCACTGCCCTC for A533V, using PfuUltra II Fusion polymerase (Agilent, Santa Clara, California, USA) and T4 ligase (New England Biolabs, Ipswich, Massachusetts, USA). Note that S508 and A533 on the $rK_{Ca}2.3$ are the equivalent positions of S507 and A532 on the $hK_{Ca}2.3$ channel. Competent *Escherichia coli* were transformed using an aliquot of the mutagenesis product by thermic shock, and the plasmid DNA was purified using standard methods. The human intermediate conductance calcium-activated potassium channel (h**$K_{Ca}3.1$**) T250S V275A mutant was kindly donated by Dorte Strøbæk. All constructs were verified by sequencing.

Cell culture and cell preparation

To study the effect of AP14145 on the h**$K_{Ca}1.1$** and $hK_{Ca}2.x$ channels, we used four different stable HEK293 cell lines expressing $hK_{Ca}1.1$, $hK_{Ca}2.1$, $hK_{Ca}2.2$ or $hK_{Ca}2.3$ channels obtained from NeuroSearch A/S (Ballerup, Denmark). The cell lines were established as described in Strøbæk *et al.*, 2004. For the identification of the binding determinants of AP14145, WT HEK293 cells were transiently co-transfected with $rK_{Ca}2.3$ WT, $rK_{Ca}2.3$ S508T A533V, $hK_{Ca}3.1$ WT or $hK_{Ca}3.1$ T250S V275A and 0.1 μg of eGFP plasmid DNA using standard Lipofectamine™ (Thermo Fisher Scientific, Waltham, Massachusetts, USA) protocols. Between 1 and 2 days after the transfection, patch-clamp experiments were conducted. The cells were cultured in DMEM (DMEM1965, Thermo Fisher Scientific) supplemented with 26.2 mM $NaHCO_3$, 25 mM HEPES, 10 mL Glutamax (Gibco, Gaithersburg, Maryland, USA), 10% FBS (Biowest, Nuaillé, France) and 100 $U{\cdot}mL^{-1}$ of penicillin/streptomycin (Sigma-Aldrich, Munich, Germany). In the case of the stable cell lines, 100 $\mu g{\cdot}mL^{-1}$ geneticin (Gibco) was added to the medium. On the day of the experiment, cells were detached from the flask using 1 mL of Detachin™ (Amsbio,

Abingdon, UK). After being washed with calcium and magnesium-free PBS, the cells were plated on 0.5 mm diameter coverslips. In the case of inside-out patch clamps, the coverslips were treated overnight at 37°C with 50 mg·mL^{-1} poly-L-lysine (Sigma-Aldrich) to get firmer cell attachment.

Solutions

Patch-clamp experiments with $K_{Ca}2$ and $K_{Ca}3.1$ channels were conducted using symmetrical K^+ solutions. The extracellular solution contained 0.1 mM $CaCl_2$, 3 mM·$MgCl_2$, 154 mM·KCl, 10 mM· HEPES and 10 mM glucose (pH 7.4 and 285–295 mOsm). The intracellular solution contained 8.106 mM·$CaCl_2$ (final free Ca^{2+} concentration of 400 nM), 1.167 mM·$MgCl_2$, 10 mM·EGTA, 154 mM·KCl, 10 mM HEPES, 31.25/10 mM·KOH/EGTA and 15 mM·KOH (pH 7.2). In addition, to study the activation of the channel with or without the presence of AP14145, we used a range of intracellular solutions containing different free Ca^{2+} concentrations (0.01–30 μM). The composition of these intracellular solutions was determined as described in Strøbæk *et al*. (2006).

For $K_{Ca}1.1$ channels, the extracellular solution contained 2 mM·$CaCl_2$, 1 mM $MgCl_2$, 145 mM NaCl, 4 mM·KCl, 10 mM HEPES and 10 mM·glucose (pH 7.4 and 285–295 mOsm). The intracellular solution contained 5.374 mM $CaCl_2$ (final free Ca^{2+} concentration of 100 nM), 1.75 mM $MgCl_2$, 120 mM·KCl, 10 mM· HEPES and 31.25/10 mM KOH/EGTA (pH 7.2).

The osmolarity of the intracellular solutions was adjusted using sucrose (Sigma-Aldrich) to match the extracellular solutions.

Electrophysiology

Patch-clamp recordings were made using a HEKA EPC9 amplifier and the Patchmaster software (HEKA Elektronik, Ludwigshafen, Germany) at room temperature. Patch pipettes were pulled using a horizontal DMZ Universal Puller (Zeitz, Germany) with resistances of 2.5 ± 0.1 MΩ for whole-cell patch clamp and 2.2 ± 0.6 MΩ for inside-out patch clamp. $K_{Ca}2$ and $K_{Ca}3.1$ currents were elicited every 2 s using a 200 ms voltage ramps ranging from −80 to +80 mV from a holding potential of 0 mV. $K_{Ca}1.1$ currents were elicited every 2 s using a 200 ms voltage ramps ranging from −80 to +50 mV from a holding potential of 0 mV. Data were sampled at 10 kHz. Series resistance values were 5.4 ± 0.6 MΩ with 80% of compensation. Two Bessel filters of 10 and 2.9 kHz were used to avoid background noise.

Plasma protein binding

Plasma protein binding (PPB) was experimentally determined by Syngene International in rat plasma using rapid equilibrium dialysis.

Animal experiments

All animal care and experimental procedures, *ex vivo* and *in vivo,* were performed under a licence from the Danish Ministry of Justice (licence no. 2013-15-2934/00964) and in accordance with the Danish guidelines for animal experiments according to the European Commission Directive 86/609/EEC. Animal studies are reported in compliance with the ARRIVE guidelines (Kilkenny *et al*., 2010; McGrath and Lilley, 2015). The animals were housed in groups of 2–4 in high-top cages with bedding (wood shavings) and under constant climatic conditions (22°C) at the Department of Experimental Medicine, University of Copenhagen. The animals were kept at a 12 h light–dark cycle with *ad libitum* access to clean water and standard laboratory rodent diet.

Isolated perfused heart preparation. Rats express $K_{Ca}2$ channels in the atria and have previously been used to study the effect of inhibiting these channels on atrial refractoriness. Male Sprague–Dawley rats (250–350 g, 1–3 months old, Janvier Labs, Le Genest-Saint-Isle, France) were anaesthetized with fentanyl-midazolam mixture, 5 mg·mL^{-1} dose 0.3 mL per 100 g, s.c. A tracheotomy was performed in the ventilated rat. The aorta was cannulated, and the heart was excised and connected to a Langendorff retrograde perfusion system (Hugo Sachs Elektronik, Harvard Apparatus GmbH, March-Hugstetten , Germany). The heart was retrogradely perfused with Krebs–Henseleit buffer (in mM: NaCl 120.0, $NaHCO_3$ 25.0, KCl 4.0, $MgSO_4$ 0.6, NaH_2PO_4 0.6, $CaCl_2$ 2.5 and glucose 11.0, saturated with 95% O_2 and 5% CO_2, 37°C, pH 7.4) at a constant perfusion pressure of 80 mmHg. The electrical activity of the heart was measured by volume conducted ECGs and the atrial epicardial monophasic action potentials by an electrode on the right atrium. The signal was sampled at 1 kHz (PowerLab Systems, ADInstruments, Oxford, UK) and monitored by using LabChart 7 software (ADInstruments). The hearts were immersed into a temperature-controlled and carbonated bath containing Krebs–Henseleit buffer. A bipolar pacing electrode was placed on the right atria in order to stimulate the heart and measure the AERP, which was defined as the longest S1–S2 interval failing to elicit an action potential. The AERP was measured every 5 min by applying electrical stimulation (two times rheobase) with a fixed interval of 133 ms (S1 stimulation), and for every 10th beat, an extra stimulus (S2 stimulation) was applied with 1 ms increments.

Baseline recordings were made for at least 20 min and continued until the ECG morphology and AERP recording were stable. After the baseline recording, four 20 min episodes followed in which the heart was perfused with (i) 1 μM·L^{-1} paxilline, (ii) 3 μM·L^{-1} paxilline, (iii) washout and (iv) 10 μM·L^{-1} AP14145, and AERP measurements were performed every fifth minute. Measurements after 20 min of drug perfusion or washout were used for statistical analysis.

In vivo experiments

Closed chest recording of atrial refractoriness in rats. A total of eighteen 1- to 3-month-old male Sprague–Dawley rats (Janvier Labs) weighing 400–550 g were anaesthetized and randomly divided in three groups: one group receiving AP14145 as bolus injections (n = 6), a time-matched control group receiving vehicle as bolus injections (n = 6) and a group receiving AP14145 as a constant-rate infusion (n = 6). The rats were anaesthetized with 3% isoflurane/oxygen, and an i.v. catheter was placed in the femoral vein for drug injection. Needle ECG electrodes were placed in each limb for ECG recordings (ADInstruments). The temperature of the rats was monitored and kept stable during the experiment with a heating lamp (37°C). A catheter with

eight electrodes (Millar Inc., Houston, Texas, USA) was placed in the right atrium of an anaesthetized rat *via* the jugular vein. Two of the electrodes were used to pace the atrium, and six electrodes were used to measure the electrical activity in the atrium. This combination allows measurements of the AERP and the changes in AERP as a consequence of injection of the test compound. Once the experiment was completed, rats were euthanized by a mixture of 200 mg·mL^{-1} pentobarbital and 20 mg·mL^{-1} lidocaine hydrochloride (Glostrup Apotek, Glostrup, Denmark) i.v. injection. As the risk of placebo effect and subjective interpretation of the results was nonexistent or minimal, no blinding was used.

Measurement of AERP. Each experiment lasted for at least 60 min and was divided into three 20 min episodes. During the entire experiment, the ECG was monitored. The AERP was measured by applying electrical stimulation (five times rheobase) with a fixed interval of 120 ms (S1 stimulation), and for every 10th beat, an extra stimulus (S2 stimulation) was applied with 1 ms increments. The AERP was defined as the longest S1–S2 interval failing to elicit an action potential. Between the AERP recordings, the heart remained unpaced. Baseline AERP recordings with no compound present were made every fifth minute for 20 min before adding test compound.

Increasing bolus dosing. After the baseline recording, two 20 min episodes followed in which two groups of rats (n = 6 each) were injected with increasing doses of AP14145 (2.5 and 5.0 mg·kg^{-1}) or equivalent volumes of vehicle (50% PEG-400 and 50% saline). The injection time was 30 s. AERP was measured 1, 5, 10 and 15 min after the start of each injection.

Constant rate infusion of AP14145. After the baseline recording, a third group of rats received a constant rate infusion of 40 mg·kg^{-1}·h^{-1} AP14145 over 20 min followed by a 20 min post-infusion period. In these animals, the AERP was measured every 2 min during and after infusion.

Beam walk test – assessment of motor balance and coordination in mice. A beam walk test was performed in mice in order to assess the effects of $K_{Ca}2$ channel inhibitors on the CNS, *in vivo*. The mouse beam walk test is a validated test for addressing motor function (Brooks and Dunnett, 2009). Three groups of 1- to 2-month-old male NMRI mice (Glostrup Taconic Biosciences, Hudson, New York, USA) weighing 23–49 g were used. The mice were randomly assigned to either the vehicle control group, a 10 mg·kg^{-1} NS8593 or a 10 mg·kg^{-1} AP14145 group. The mice were placed on a 1 m wooden beam (12 mm diameter) and briefly trained in crossing the beam. After training, a 1 min baseline recording was initiated, and the number of falls and slips was noted. Hereafter, the mice were randomly assigned to receive $K_{Ca}2$ channel inhibitors or vehicle (50% PEG-400 and 50% saline) by i.v. bolus injection in the tail vein. The mouse was observed immediately after injection for any behavioural changes. If any adverse effects occurred, the mouse was killed. Otherwise, the mice were observed for behavioural changes and challenged with the beam walk 12 min post-injection. All experiments were documented by video recordings.

Data and statistical analysis

The data and statistical analysis comply with the recommendations on experimental design and analysis in pharmacology (Curtis *et al.*, 2015). Data were extracted from PatchMaster and analysed using GraphPad Prism 7. To calculate the IC_{50} value of AP14145, the measured currents were first normalized. Recorded currents without the presence of the drug were used as baseline, and currents recorded at the highest tested concentration of AP14145 (30 μM·L^{-1}) were used as total inhibition of the channel. Individual IC_{50} values for each experiment were calculated using the equation:

$$Y = Y_{min} + \frac{(Y_{max} - Y_{min})}{1 + 10^{X - \log IC_{50}}}$$

where X is the log of dose of AP14145 and Y is the normalized measured current. In all cases, a Hill slope of −1.0 was considered. Individual IC_{50} values were later used to obtain the final $\bar{x}$ ± SEM IC_{50}. The individual IC_{50} values were then used in Student's t-tests to determine subtype selectivity.

To calculate the EC_{50} of calcium, the values were normalized using the currents recorded at the lowest calcium concentration (0.01 μM·L^{-1}) for total inactivation and at the highest calcium concentration (30 μM·L^{-1}) for maximum activation of the channel. Individual EC_{50} values for each experiment were calculated using the equation:

$$Y = Y_{min} + \frac{(Y_{max} - Y_{min})}{1 + 10^{(\log EC_{50} - X) \times \text{Hill slope}}}$$

where X is the log of dose of calcium and Y is the normalized measured current with variable Hill slope. Individual EC_{50} values were used to determine the final EC_{50}, as means ± SEM.

Currents were also normalized to assess and compare the inhibitory effect of 10 μM·L^{-1} AP14145 on HEK cells expressing $K_{Ca}1.1$, $K_{Ca}2.1$, $K_{Ca}2.2$, $K_{Ca}2.3$, $K_{Ca}2.3$ S508T A532V, $K_{Ca}3.1$ or $K_{Ca}3.1$ T250S V275A. For each individual cell, 0% current was defined as 0 nA, and 100% current was defined as the current recorded in the absence of the compound. The final results are summarized as means ± SEM of the individual values. To quantify and compare the activation and inhibition effects of 10 μM·L^{-1} NS309 and 10 μM·L^{-1} AP14145 on the $K_{Ca}2.3$ channels, values were normalized for each individual cell. In this case, 0 was defined as 0 nA, and currents recorded in the absence of both compounds were defined as 1. These individual values were used to calculate the final $\bar{x}$ ± SEM.

The last 10 data points obtained after the application of a new compound or solution and corresponding to the steady state were used to create every single value. Student's t-test was performed to assess statistical significance of the effect of AP14145. Values of P <0.05 were considered significant.

Perfused rat heart data and closed chest continuous data are summarized using the means ± SEM. A one-way ANOVA with Tukey's comparison post test was used to compare the effect of paxilline and AP14145 on the isolated rat heart. Multiple t-tests with Holm–Sidak's correction for multiple comparisons were used to compare AERP differences between the group of rats that received AP14145 as increasing bolus doses and the time-matched control group at matching time

points. Multiple *t*-tests with Holm–Sidak's correction for multiple comparisons were used to compare each AERP-value during and after infusion to the mean baseline AERP values. *P* values <0.05 were considered significant.

Physicochemical properties of AP14145 and NS8593 were calculated using the Instant JChem (ChemAxon, Budapest, Hungary) software.

Materials

AP14145 (*N*-(2-{[(1*R*)$^{-1}$-[3-(trifluoromethyl)phenyl]ethyl]amino}$^{-1}$*H*$^{-1}$,3-benzodiazol-4-yl)acetamide) was synthetized by Syngene International (Bangalore, India) as described in the relevant Patent WO 2013104577 A1. For *in vitro* experiments, AP14145 was solubilized in pure DMSO (Sigma-Aldrich) at 10 mM· stock solutions. These stock solutions were stored at −20°C, and aliquots were solubilized at the desired concentration on the day of the experiment. For *in vivo* experiments, 5 mg·mL^{-1} AP14145 was dissolved in a vehicle consisting of 50% polyethylene glycol (PEG) 400 (Merck, Darmstadt, Germany) and 50% sterile saline (PanReac AppliChem, Darmstadt, Germany) for infusion, and the solution was sterile filtered (Nalgene, rapid flow 90 mm·filter unit, Thermo Fisher Scientific) before use. The K_{Ca}1.1 channel selective inhibitor **paxilline** was purchased from Sigma-Aldrich. NS8593 and NS 309 was supplied by NeuroSearch A/S, Ballerup, Denmark.

Nomenclature of targets and ligands

Key protein targets and ligands in this article are hyperlinked to corresponding entries in http://www.guidetopharmacology.org, the common portal for data from the IUPHAR/BPS Guide to PHARMACOLOGY (Southan *et al.*, 2016), and are permanently archived in the Concise Guide to PHARMACOLOGY 2015/16 (Alexander *et al.*, 2015a,b).

Results

AP14145 inhibits both hK$_{Ca}$2.2 and hK$_{Ca}$2.3 channel currents with equal potency

Using inside-out manual patch clamps, we tested AP14145 on both the hK$_{Ca}$2.2 and hK$_{Ca}$2.3 channels. Once the patch was excised, the channels were exposed to the bath's intracellular solution, containing 400 nM·free Ca^{2+}. In symmetrical intracellular and extracellular K^+ solutions, hK$_{Ca}$2.3 currents displayed a characteristic inwardly rectifying current–voltage relationship (Figure 2A). Currents were elicited using voltage ramps from −80 to +80 mV applied every 2 s. Once the hK$_{Ca}$2 current was stable, up to eight increasing concentrations of AP14145 between 0.01 and 30 μM·were applied and perfused by gravity flow on the patch (Figure 2B). For each concentration, the drug was applied until steady state was reached.

AP14145 was able to inhibit both hK$_{Ca}$2.2 and hK$_{Ca}$2.3 channel currents in a concentration-dependent fashion (Figure 2B, data not shown for hK$_{Ca}$2.2). The effect started at nM concentrations and total inhibition was reached at 30 μM (Figure 2B). Calculated IC_{50} for AP14145 on both the hK$_{Ca}$2.2 and hK$_{Ca}$2.3 currents was 1.1 ± 0.3 μM (n = 7 each, Figure 2C), with a fixed Hill slope of −1.0. The drug consequently did not display any subtype selectivity between hK$_{Ca}$2.2 and hK$_{Ca}$2.3 channels.

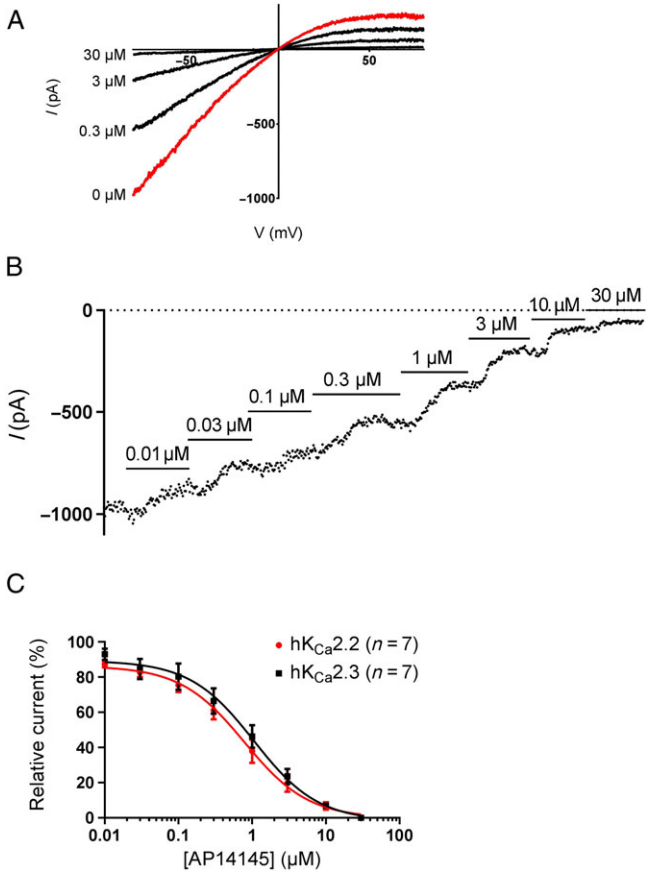

Figure 2

(A) Representative current–voltage recordings of the inhibition of hK$_{Ca}$2.3 channels by increasing concentrations of the drug AP14145 and (B) its current–time plot obtained by inside-out patch clamp on HEK cells stably expressing the channel. (C) Inhibition curves of AP14145 on both the hK$_{Ca}$2.2 (n = 7) and hK$_{Ca}$2.3 (n = 7) channel.

Additionally, the inhibitory effect of AP14145 was also tested on the hK$_{Ca}$1.1, hK$_{Ca}$2.1 and hK$_{Ca}$3.1 channels using whole-cell patch clamp for further selectivity assessment (Figure 3). The application of 10 μM·AP14145 inhibited 50 ± 10% of the hK$_{Ca}$1.1 current (n = 6) and 90 ± 4% of the hK$_{Ca}$2.1 current (n = 7). In contrast, hK$_{Ca}$3.1 channel currents were not significantly affected by the application of 10 μM AP14145 (n = 8).

AP14145 modifies calcium sensitivity of hK$_{Ca}$2.3 channels

To establish how AP14145 inhibits the channel, we performed inside-out patch-clamp recordings to assess the effect of the drug on the calcium sensitivity of the hK$_{Ca}$2.3 channel. Patches were excised from HEK cells stably expressing the hK$_{Ca}$2.3 channel, and currents elicited using voltage ramps. We exposed the patches to eight different free Ca^{2+} concentrations and calculated the EC_{50} for calcium activation of the channel in the absence and presence of 10 μM AP14145 (Figure 4A, B). Free calcium concentrations ranged from

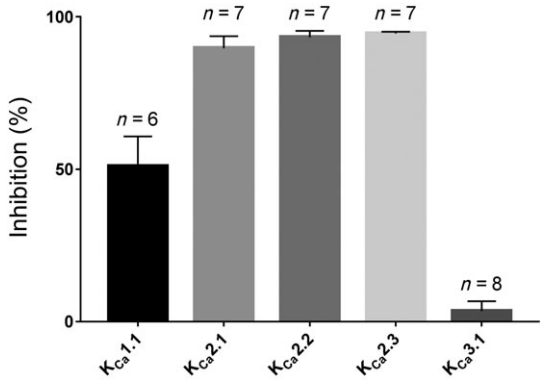

Figure 3

Inhibitory effect of 10 μM·AP14145 on $K_{Ca}1.1$, $K_{Ca}2.1$, $K_{Ca}2.2$, $K_{Ca}2.3$ and KCa3.1 channels. All measurements were obtained by whole-cell patch clamp except $K_{Ca}2.2$ channels, which were obtained by inside-out patch clamp.

0.01 to 30 μM and were perfused using gravity flow. Solutions were applied until steady state was reached.

In the absence of AP14145, $hK_{Ca}2.3$ channels were fully activated at 3 μM·of intracellular Ca^{2+} (Figure 4A), but in the presence of 10 μM AP14145, up to 10 μM·Ca^{2+} was needed to reach total activation of the channel (Figure 4B). At 10 μM·, the drug shifted the calcium-activation curve of the $K_{Ca}2.3$ channel to the right (Figure 4C), so higher calcium concentrations were needed to activate the channels. This was also shown by the significant increase of the EC_{50} of Ca^{2+} from 0.36 ± 0.02 (n = 9) to 1.3 ± 0.2 μM (n = 7). Most prominently, the Hill coefficients were also significantly modified by AP14145, from a control value of 5.2 ± 0.3 to 1.2 ± 0.1 in the presence of 10 μM·AP14145.

AP14145 reverses the effect of a positive gating modulator of $K_{Ca}2$ channels, NS309

The inhibitory effect of AP14145 was also studied in the presence of a high concentration of the $K_{Ca}2$ positive gating modulator **NS309**. Patches excised from HEK cells stably expressing the $hK_{Ca}2.3$ channel were exposed to intracellular solutions containing 400 nM·free Ca^{2+}. After stabilization of the baseline, 10 μM NS309 was applied on the patch, further activating the channel and increasing $hK_{Ca}2.3$ current by 4 ± 1-fold (n = 7, Figure 5). When steady state was reached, 10 μM·AP14145 was added to the bath, in the continued presence of NS309. The application of AP14145 reduced $hK_{Ca}2.3$ current to values close to the control baseline, reversing the positive gating effect of NS309 (Figure 5). Furthermore, in the presence of 10 μM NS309, total current inhibition by 10 μM·AP14145 was significantly diminished from 80 ± 3 (n = 7) to 61 ± 4% (n = 7, Figure 5).

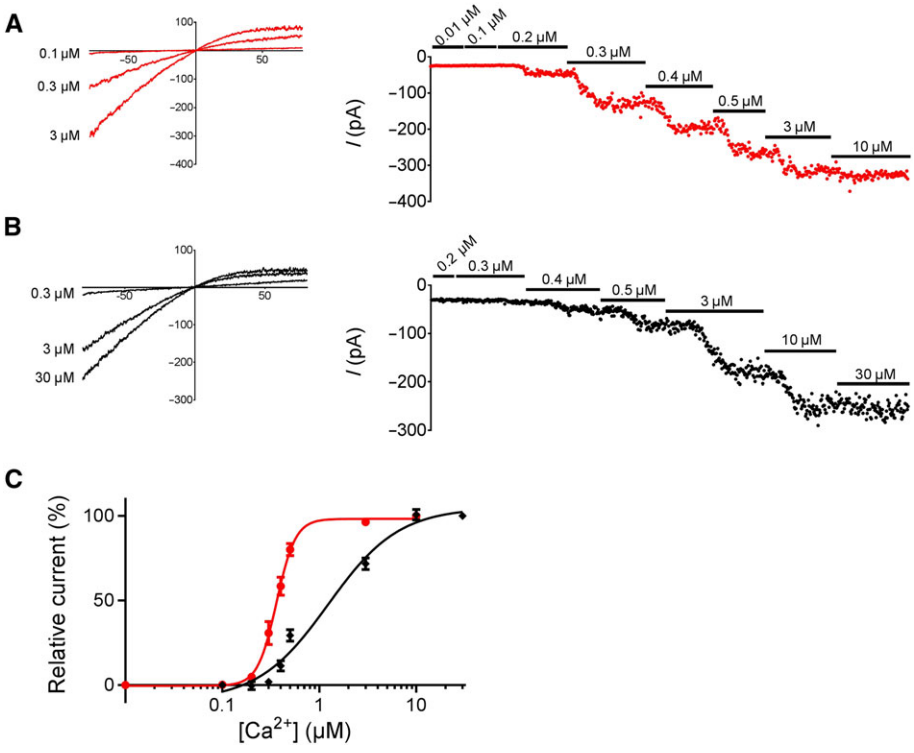

Figure 4

Representative current–voltage plots (left) and their corresponding current–time plots (right) of activation by calcium of $hK_{Ca}2.3$ channels (A) in the absence of AP14145 and (B) in the presence of 10 μM·AP14145. (C) Calcium activation curves for the $hK_{Ca}2.3$ channel in the absence of AP14145 (n = 9) and in the presence of 10 μM·AP14145 (n = 7).

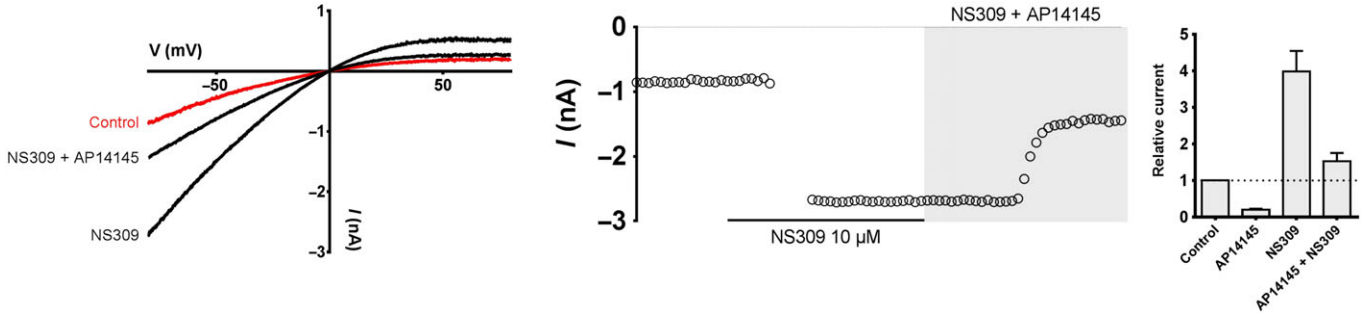

Figure 5

Representative current–voltage plot (left) and its corresponding current–time plot (centre) of the effect of 10 μM·NS309 in the absence and in the presence of 10 μM·AP14145 on excised hK$_{Ca}$2.3 patches. On the right, bar graph comparing the effects of 10 μM AP14145 (n = 7), 10 μM·NS309 (n = 7) and 10 μM AP14145 + 10 μM·NS309 (n = 7) on excised hK$_{Ca}$2.3 patches.

AP14145 inhibition strongly depends on two amino acids, S508 and A533, located in the inner pore of the channel

To establish possible molecular determinants of rK$_{Ca}$2.3 inhibition by AP14145, we mutated two amino acids, S508 and A533 (corresponding to S507 and A532 in hK$_{Ca}$2.3), located in the inner pore of the channel and known to confer sensitivity to the negative allosteric modulator of K$_{Ca}$2 channels, NS8593 (Jenkins *et al.*, 2011).

Whole-cell patch-clamp experiments were conducted on transiently transfected HEK cells with either the WT rK$_{Ca}$2.3 channel or the rK$_{Ca}$2.3 S508T A533V mutant. The channels were activated by 400 nM·free Ca^{2+} in the intracellular solution, and currents were elicited using voltage ramps. Again, in symmetrical intracellular and extracellular K^+ solutions, WT rK$_{Ca}$2.3 currents displayed a characteristic inwardly rectifying current–voltage relationship (Figure 6A). In contrast to the WT rK$_{Ca}$2.3 channel, the maximum current normalized to cell capacitance of the mutant rK$_{Ca}$2.3 was significantly reduced (WT: 650 ± 96 pA·pF^{-1} vs. mutant: 87 ± 23 pA·pF^{-1}, n = 7 each, Figure 6B). Rectification, determined as the ratio of the current amplitude at −80 and +80 mV, was also changed by the mutation, from 9 ± 1 I_{-80}/I_{+80} in the WT to 2.9 ± 0.4 I_{-80}/I_{+80} in the mutant. These observations are in agreement with the results previously described by Jenkins *et al.*, 2011. After current stabilization, 10 μM·of AP14145 was applied on the cell transfected with the WT or the mutant protein for 1–2 min or until a steady-state drug effect was reached (Figure 6A, B).

The experiments showed that, while rK$_{Ca}$2.3 currents recorded from cells transfected with the WT channel were strongly inhibited by application of 10 μM·AP14145 (Figure 6A), currents recorded from cells transfected with the mutant rK$_{Ca}$.2.3 channel were only partly affected by the presence of the compound (Figure 6B). The inhibitory effect of AP14145 was statistically different between the WT and the S508T A533V mutant when analysed as the relative current inhibition after application of AP14145 (Figure 6E).

To comfirm that the two residues, S508 and A533, were important for AP14145 sensitivity, we introduced these amino acids in their homologous positions in the AP14145 insensitive K$_{Ca}$3.1 channel, T250 and V275 respectively. The K$_{Ca}$3.1 T250S V275A mutant was tested using whole-cell patch clamp to determine its sensitivity to AP14145. After activation of the channel with 400-nM·L^{-1} free Ca^{2+} intracellular solution and current stabilization, 10 μM·AP14145 was applied to the cell. In contrast to the K$_{Ca}$3.1 WT channel (Figure 6C), the mutant K$_{Ca}$3.1 current was inhibited by 92 ± 1% (n = 7, Figure 6D), comparable with the inhibitory effect observed on rK$_{Ca}$2.3 channels.

AP14145 increases the duration of the atrial effective refractory period (AERP) in isolated perfused rat hearts

Excised rat hearts were connected to a retrograde Langendorff perfusion system to measure the effect of AP14145 on the AERP and discount any effects mediated by K$_{Ca}$1.1 channels.

Once a stable baseline was achieved, the hearts were perfused first with 1 μM·of the K$_{Ca}$1.1 channel inhibitor paxilline. Twenty minutes later, the concentration of paxilline was increased to 3 μM·for 20 more minutes. Finally, after a 20 min wash period, 10 μM· of AP14145 was perfused into the heart. As shown in Figure 7, paxilline did not affect the AERP in any of the tested doses, but AP14145 was able to prolong the AERP significantly.

AP14145 increases the duration of the atrial effective refractory period in rats

To investigate the *in vivo* effects of AP14145, six male rats received AP14145 in increasing doses (2.5 and 5 mg·kg^{-1}), and six time-matched control rats received corresponding volumes of vehicle (0.5 and 1 mL·kg^{-1}, respectively).

One minute after injection of 2.5 mg·kg^{-1} AP14145, the AERP was significantly increased (Figure 8A). The AERP returned towards baseline values, and 5 min after the injection of 2.5 mg·kg^{-1}, the AERP was no longer significantly different from that of the time-matched controls. One minute after injection of 5 mg·kg^{-1} AP14145, the AERP was significantly increased from 31 ± 2 ms in the time-matched control group to 58 ± 8 ms (Figure 8A). Again, the AERP returned towards baseline values, and 10 min after the injection of 5 mg·kg^{-1}, the AERP was no longer significantly different from that of the time-matched controls.

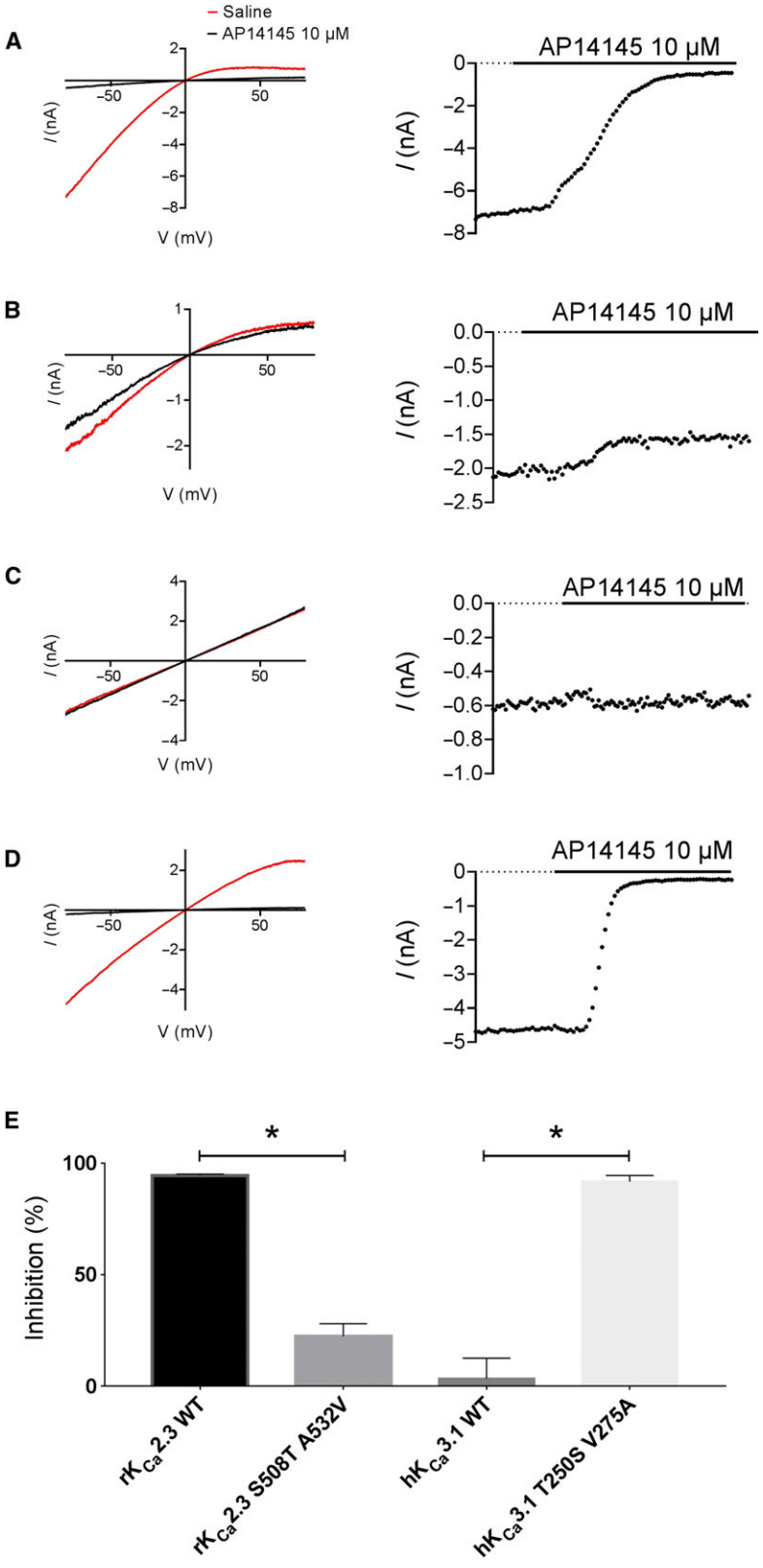

Figure 6

Representative current–voltage plots (left) and current–time plots (right) depicting the effect of AP14145 10 μM·on HEK cells transiently transfected with (A) rKCa2.3 WT, (B) rK$_{Ca}$2.3 S508T A533V, (C) hK$_{Ca}$3.1 WT and (D) hK$_{Ca}$3.1 T250S V275A recorded using whole-cell patch clamp. (E) Bar graph comparing the inhibitory effect of 10 μM·AP14145 on rK$_{Ca}$2.3 WT ($n = 7$), rK$_{Ca}$2.3 S508T A533V ($n = 7$), hK$_{Ca}$3.1 WT channel ($n = 8$) and hK$_{Ca}$3.1 T250S V275A ($n = 7$). *$P<0.05$, significantly different as indicated.

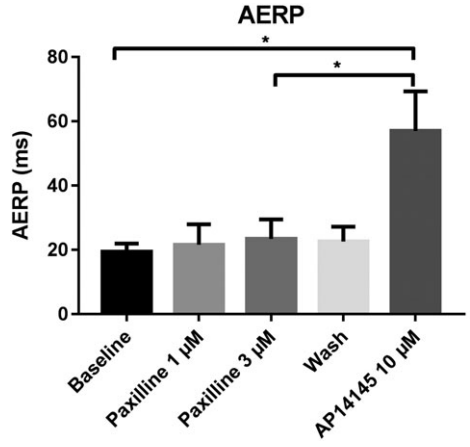

Figure 7

Effect of 1 and 3 µM·of the $K_{Ca}1.1$ channel inhibitor paxilline and 10-µM·AP14145 on the AERP of isolated perfused rat hearts (n = 5). *P<0.05, significantly different as indicated.

A third group of rats (n = 6) received a constant rate infusion of 40 mg·kg^{-1}·h^{-1} over 20 min and was monitored for an additional 20 min after infusion (Figure 8B). In these rats, the AERP was significantly increased compared with baseline values from 4 min after the infusion started (i.e. after a cumulative dose of 2.7 mg·kg^{-1}). The AERP continued to increase during the rest of the infusion and returned towards baseline values after infusion.

AP14145 does not impair motor coordination in mice

A beam walk test was performed in mice in order to assess the CNS effects of $K_{Ca}2$ channel inhibitors *in vivo*. Three groups of male NMRI mice were used, a vehicle control group (30.5 ± 0.3 g, n = 6), a 10 mg·kg^{-1} NS8593 (26 ± 1 g, n = 3) and a 10 mg·kg^{-1} AP14145 group (36 ± 5 g, n = 6).

Shortly after the injection of 10 mg·kg^{-1} NS8593, all mice showed severe convulsions making them unable to walk on the beam (Figure 9). Therefore, the mice were killed by cervical dislocation, and the experiment was terminated.

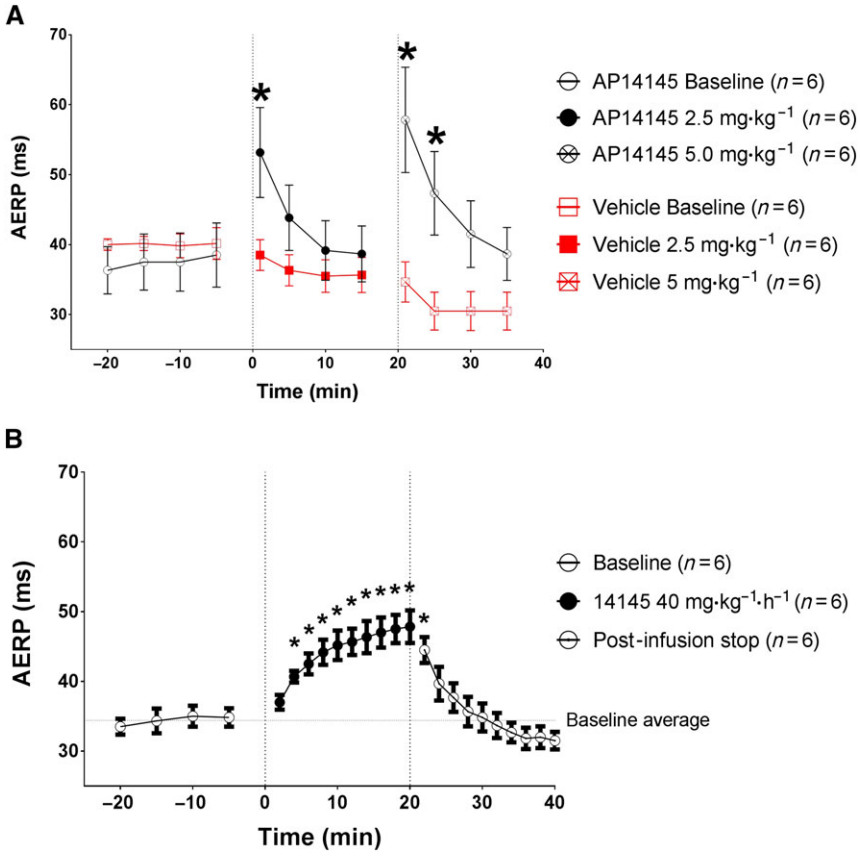

Figure 8

Effects on AERP in closed chest *in vivo* rats. (A) Bolus doses of 2.5 and 5 mg·kg^{-1} AP14145 significantly increased the AERP compared with time-matched controls receiving corresponding volumes of vehicle. (B) AP14145 given as a constant rate infusion of 40 mg·kg^{-1}·h^{-1} over 20 min increased AERP compared with the baseline average and returned towards baseline values post-infusion. *P<0.05, significantly different from (A) corresponding vehicle values, (B) baseline values.

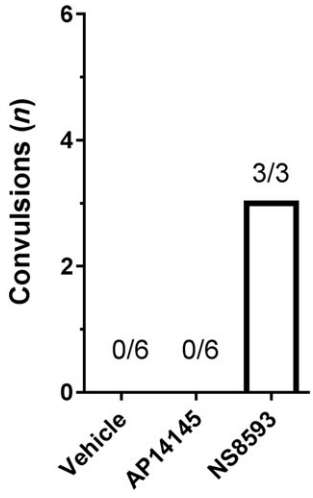

Figure 9

Bar graph depicting the number of convulsions triggered by the administration of the vehicle, 10 mg·kg^{-1} AP14145 and 10 mg·kg^{-1} NS8593.

In contrast, when mice were injected with AP14145, no acute effects were observed, and the beam walk test was performed 12 min after dosing. The mice did not slip or fall from the beam in either of the two tests, and no behavioural changes were observed. These observations were not different from those of the vehicle control group (Figure 9).

Discussion

$K_{Ca}2$ channels are inwardly rectifying potassium channels (Köhler *et al.*, 1996) widely distributed in humans, both in the CNS and peripheral tissues (Chen *et al.*, 2004). In the heart, they play an important role in the late repolarization phase of the atria (Li *et al.*, 2009). Moreover, inhibition of $K_{Ca}2$ channels prolongs the AERP (Diness *et al.*, 2010; Skibsbye *et al.*, 2011; Qi *et al.*, 2014; Haugaard *et al.*, 2015). Therefore, the $K_{Ca}2$ channel is considered a promising new target to treat AF. Here, we present a new $K_{Ca}2$ channel inhibitor, AP14145, which could constitute an important tool in rodents, to target and study the inhibition of peripheral $K_{Ca}2.x$ channels *in vivo*.

In initial experiments, AP14145 inhibited $hK_{Ca}2.2$ and $hK_{Ca}2.3$ channels in an equipotent manner with IC_{50} values of 1.1 ± 0.3 μM. To determine the mechanism of inhibition of AP14145, we conducted inside-out patch-clamp experiments. Patches were excised from HEK 293 cells stably expressing the $hK_{Ca}2.3$ channel and exposed to a range of intracellular solutions with different free calcium concentrations. Calcium activation was assessed in the absence and presence of AP14145. The compound significantly increased the EC_{50} of Ca^{2+} from 0.36 ± 0.02 to 1.3 ± 0.2 μM·L^{-1}, thereby shifting the Ca^{2+} activation curve of $K_{Ca}2$ channels to higher values. The Hill coefficients were also modified by the presence of AP14145 from 5.2 ± 0.3 (control) to 1.2 ± 0.1 (10 μM·AP14145). These results suggest that the drug modifies the calcium sensitivity of the channel and acts as a negative allosteric modulator, very similar to the previously reported NS8593. The change of the Hill coefficient may also indicate a loss of calcium cooperativity that may impede calcium binding. Moreover, the inhibitory effect of AP14145 was studied in the presence of the $K_{Ca}2.x$ positive allosteric modulator NS309, which is known to increase the calcium sensitivity of the channel (Strøbæk *et al.*, 2004). In these experiments, AP14145 was able to reverse NS309-mediated $K_{Ca}2.3$ channel activation, suggesting a functional competition between the two compounds and further supporting the a negative allosteric mechanism of action for AP14145.

In the study by Jenkins *et al.* (2011), the binding site of NS8593, another $K_{Ca}2$ negative allosteric modulator, was located at the inner pore of the channel. This was an interesting finding since the drug had previously been found to decrease calcium sensitivity of the channel and its binding site was tentatively located in the C-terminal domain, close to the calmodulin-binding domain. Instead, in our experiments, binding of AP14145 involved interactions with two specific amino acid residues, S507 and A532, located on helixes S5 and S6 respectively. When these two amino acids were mutated to the corresponding residues found on the closely related $K_{Ca}3.1$ channel, which is not inhibited by NS8593, the resulting $K_{Ca}2.3$ channel mutant was resistant to the effect of the drug, with preserved channel confirmation and calcium sensitivity. In order to find out if AP14145 and NS8593 shared the same binding site, we conducted whole-cell patch-clamp experiments on transiently transfected HEK cells with $rK_{Ca}2.3$ WT or $rK_{Ca}2.3$ S508T A533V, corresponding to S507 and A532 in the $hK_{Ca}2.3$ channel. While the WT current was strongly inhibited using 10 μM AP14145, the NS8593 resistant mutant was only partially affected by the presence of the drug, suggesting that S508 and A533 are important also for AP14145 inhibition. The loss of AP14145 sensitivity in $rK_{Ca}2.3$ S508T A533V cannot be explained by differences in calcium-activation or channel conformation as these characteristics are preserved in the mutant (Jenkins *et al.*, 2011). AP14145 and NS8593 are structurally close analogues (Figure 1), and these experiments demonstrate that AP14145 and NS8593 appear to share the same inhibition mechanism as well as some of their binding determinants. Finally, to confirm that S507 and A532 are important for the inhibitory effect of AP14145 on $K_{Ca}2.3$, we introduced these amino acids in their homologous positions on the $K_{Ca}3.1$ channel, which is not sensitive to the effects of AP14145. With the addition of these two amino acids, AP14145 sensitivity was fully restored in the $K_{Ca}3.1$ channel (Figure 6), further demonstrating that S507 and A532 are important for AP14145 inhibition. $K_{Ca}2$ channels are widely expressed in the brain, including the cerebellum (Stocker and Pedarzani, 2000), where they contribute to the action potential afterhyperpolarization (Hosy *et al.*, 2011). Further, inhibition of $K_{Ca}2.2$ channels in cerebellum disturbs the motor output and this action is manifested as ataxia or a convulsion-like phenotype, especially apparent in the hind legs (Alvina and Khodakhah, 2010). As an indication of CNS exposure and inhibition of central $K_{Ca}2$ channels, a beam walk test was performed. The test is designed to assess impaired motor coordination and balance in mice.

Mice injected i.v. with 10 mg·kg^{-1} NS8593 immediately showed acute CNS effects in the form of convulsions and consequently were immediately killed. In contrast, i.v. injection of 10 mg·kg^{-1} AP14145 had no apparent CNS effects, and the treated mice were able to cross the beam without slipping or falling from the beam, similarly to the vehicle control mice. Importantly, binding of NS8593 to plasma protein is higher than that of AP14145 (95.38 vs. 91.35% bound, respectively, Table 1). Thus there is more AP14145 available as free drug in plasma, compared with NS8593, when the same dose of both compounds is injected. Moreover, we found that i.v. injection of 2.5 mg·kg^{-1} AP14145 significantly increased the atrial refractoriness in rats within 1 min of injection, suggesting that 10 mg·kg^{-1} would be sufficient to block the peripheral $K_{Ca}2$ channels.

A possible explanation for the apparent difference in CNS penetration of the two compounds lies in their structure (Figure 1) and physicochemical properties (Table 1). In particular, AP14145 contains a carboxamide moiety on the bicyclic benzimidazole ring, a chemical moiety that adds polarity to the molecule and is known to be a common substrate for **P-glycoprotein transporter**-mediated efflux. The calculated polar surface area of AP14145 is 70, which is significantly higher than that of NS8593 (Table 1), indicating a lower likelihood of penetrating the blood–brain barrier. It is thus possible that the structural features in AP14145 make the compound less likely to penetrate the BBB and to induce CNS-mediated convulsions, compared with NS8593. Although this difference in profile could in principle be caused by differences in the pharmacokinetic profile of the two compounds, this seems an unlikely explanation, because, as has been shown in Diness *et al*. (2010), 5 mg·kg^{-1} NS8593 causes similar increases of the AERP in rats when compared with the effect of 5 mg·kg^{-1} AP14145 (Figure 8A).

High concentrations of AP14145 (10 μM) significantly inhibited the $K_{Ca}1.1$ channel. However, as paxilline, which is a well-known specific inhibitor of $K_{Ca}1.1$ channels (Nardi and Olesen, 2008), did not have any effect on the atrial refractoriness of isolated perfused rat hearts, we conclude that the inhibition of $K_{Ca}1.1$ channels by AP14145 does not contribute to the AERP prolonging effects of AP14145. This is in accordance with studies demonstrating the lack of $K_{Ca}1.1$ channels and currents in the plasma membrane of cardiomyocytes (Bautista *et al*., 2009; Singh *et al*., 2013).

The apparent reduced CNS exposure of the drug makes AP14145 a unique and useful new tool compound that allows the study of peripheral $K_{Ca}2$ inhibition without apparently interfering with CNS function in awake rodents. This should help further development and understanding of the cardiac and endothelial role of $K_{Ca}2$ channels in a number of physiological and pathological settings.

In conclusion, we describe here the novel $K_{Ca}2$ channel negative gating modulator AP14145. This new compound inhibits both the $hK_{Ca}2.2$ and $hK_{Ca}2.3$ channels with equal potency (IC_{50} = 1.1 ± 0.3 μM·with 400 nM intracellular Ca^{2+}) by decreasing the calcium sensitivity of the channel. The inhibitory effect of AP14145 is strongly dependent on two amino acids, S508 and A533 in the $rK_{Ca}2.3$ channel, located in the inner pore of the channel. *In vivo*, AP14145 significantly increases atrial refractoriness in rats shortly after a single 2.5 or 5.0 mg·kg^{-1} bolus injection. In contrast to NS8593, a dose of 10 mg·kg^{-1} of AP14145 did not trigger any apparent acute CNS-mediated effects in mice, suggesting that the compound does not penetrate the blood–brain barrier to the same degree as NS8593 in rodents. This key difference could, for the first time, allow the use of a $K_{Ca}2$ channel negative modulator *in vivo* without interfering with CNS function. We expect this feature might help further development and understanding of the cardiac and endothelial role of $K_{Ca}2$ channels.

Table 1

Calculated physicochemical properties and plasma protein binding of NS8593 and AP14145

	log D (pH 7.4)	log P	PSA (Å^2)	PPB (% bound)
NS8593	4.0	4.1	41	95.38
AP14145	3.6	3.7	70	91.35

PSA, polar surface area; PPB, plasma protein binding.

Acknowledgements

The study was supported by Innovation Fund Denmark, the Carlsberg Foundation and the European Union's Horizon 2020 research and innovation programme under the Marie Skłodowska-Curie grant agreement no. 675351. We would also like to thank Dorte Strøbæk for kindly donating the $hK_{Ca}3.1$ T250S V275A mutant.

Author contributions

R.S.-V. contributed to the conception and design of the study, data acquisition (electrophysiology and molecular biology) and analysis, and drafting and critical revision of the work; J.E.K. and T.S. to the acquisition of data (closed chest recordings), data analysis, and drafting and critical revision of the work; L.A.J. to the acquisition of data (beam walk test and perfused heart preparation), data analysis, and drafting and critical revision of the work; B.D. to the data acquisition (electrophysiology and molecular biology) and analysis; U.S. S. to the conception and design of AP14145, conception and design of the study and drafting and critical revision of the work; M.G. to the conception and design of the study and critical revision of the work; J.G.D. to the conception and design of the study, data analysis, and drafting and critical revision of the work; and B.H.B. to the conception and design of the study and drafting and critical revision of the work.

Conflict of interest

All authors of this study are or have been employed by Acesion Pharma.

Declaration of transparency and scientific rigour

This Declaration acknowledges that this paper adheres to the principles for transparent reporting and scientific rigour of preclinical research recommended by funding agencies, publishers and other organisations engaged with supporting research.

References

Adelman JP (2016). SK channels and calmodulin. Channels 10: 1–6.

Alexander SPH, Catterall W, Kelly E, Marrion N, Peters J, Benson H *et al*. (2015a). The Concise Guide to PHARMACOLOGY 2015/16: Voltage-gated ion channels. Br J Pharmacol 172: 5904–5941.

Alexander SPH, Kelly E, Marrion N, Peters JA, Benson HE, Faccenda E *et al*. (2015b). The Concise Guide to PHARMACOLOGY 2015/16: Transporters. Br J Pharmacol 172: 6110–6202.

Alvina K, Khodakhah K (2010). K_{Ca} channels as therapeutic targets in episodic ataxia type-2. J Neurosci 30: 7249–7257.

Bautista L, Castro MJ, López-Barneo J, Castellano A (2009). Hypoxia inducible factor-2α stabilization and maxi-K^+ channel β_1-subunit gene repression by hypoxia in cardiac myocytes: role in preconditioning. Circ Res 104: 1364–1372.

Brooks SP, Dunnett SB (2009). Tests to assess motor phenotype in mice: a user's guide. Nat Rev Neurosci 10: 519–529.

Chen MX, Gorman SA, Benson B, Singh K, Hieble JP, Michel MC *et al*. (2004). Small and intermediate conductance Ca^{2+}-activated K^+ channels confer distinctive patterns of distribution in human tissues and differential cellular localisation in the colon and corpus cavernosum. Naunyn Schmiedebergs Arch Pharmacol 369: 602–615.

Christophersen IE, Rienstra M, Roselli C, Yin X, Geelhoed B, Barnard J *et al*. (2017). Large-scale analyses of common and rare variants identify 12 new loci associated with atrial fibrillation. Nat Genet 49: 946–952.

Curtis MJ, Bond RA, Spina D, Ahluwalia A, Alexander SP, Giembycz MA *et al*. (2015). Experimental design and analysis and their reporting: new guidance for publication in BJP. Br J Pharmacol 172: 3461–3471.

Diness JG, Bentzen BH, Sørensen US, Grunnet M (2015). Role of calcium-activated potassium channels in atrial fibrillation pathophysiology and therapy. J Cardiovasc Pharmacol 66: 441–448.

Diness JG, Sørensen US, Nissen JD, Al-Shahib B, Jespersen T, Grunnet M *et al*. (2010). Inhibition of small-conductance Ca^{2+}-activated K^+ channels terminates and protects against atrial fibrillation. Circ Arrhythm Electrophysiol 3: 380–390.

Ellinor PT, Lunetta KL, Glazer NL, Pfeufer A, Alonso A, Chung MK *et al*. (2010). Common variants in KCNN3 are associated with lone atrial fibrillation. Nat Genet 42: 240–244.

Habermann E (1984). Apamin Pharmac Ther 25: 255–270.

Haugaard MM, Hesselkilde EZ, Pehrson S, Carstensen H, Flethøj M, Præstegaard KF *et al*. (2015). Pharmacologic inhibition of small-conductance calcium-activated potassium (SK) channels by NS8593 reveals atrial antiarrhythmic potential in horses. Heart Rhythm 12: 825–835.

Hosy E, Piochon C, Teuling E, Rinaldo L, Hansel C, Hansel C (2011). SK2 channel expression and function in cerebellar Purkinje cells. J Physiol J Physiol S *58914* : 3433–3440.

Jenkins DP, Strobaek D, Hougaard C, Jensen ML, Hummel R, Sorensen US *et al*. (2011). Negative gating modulation by (*R*)-*N*-(benzimidazol-2-yl)-1,2,3,4-tetrahydro-1-naphthylamine (NS8593) depends on residues in the inner pore vestibule: pharmacological evidence of deep-pore gating of K(Ca)2 channels. Mol Pharmacol 79: 899–909.

Kilkenny C, Browne W, Cuthill IC, Emerson M, Altman DG (2010). Animal research: reporting *in vivo* experiments: the ARRIVE guidelines. Br J Pharmacol 160: 1577–1579.

Köhler M, Hirschberg B, Bond CT, Kinzie JM, Marrion NV, Maylie J *et al*. (1996). Small-conductance, calcium-activated potassium channels from mammalian brain. Science 273: 1709–1714.

Lam J, Coleman N, Garing LA, Wulff H (2013). The therapeutic potential of small-conductance $K_{Ca}2$ channels in neurodegeneratve and psychiatric diseases. Expert Opin Ther Targets 17: 1203–1220.

Li N, Timofeyev V, Tuteja D, Xu D, Lu L, Zhang Q *et al*. (2009). Ablation of a Ca^{2+}-activated K^+ channel (SK2 channel) results in action potential prolongation in atrial myocytes and atrial fibrillation. J Physiol 587: 1087–1100.

McGrath JC, Lilley E (2015). Implementing guidelines on reporting research using animals (ARRIVE etc.): new requirements for publication in BJP. Br J Pharmacol 172: 3189–3193.

Milkau M, Köhler R, de Wit C (2010). Crucial importance of the endothelial K^+ channel SK3 and connexin40 in arteriolar dilations during skeletal muscle contraction. FASEB J 24: 3572–3579.

Nardi A, Olesen S-P (2008). BK channel modulators: a comprehensive overview. Curr Med Chem 15: 1126–1146.

Nattel S (2002). New ideas about atrial fibrillation 50 years on. Nature 415: 219–226.

Pedarzani P, McCutcheon JE, Rogge G, Jensen BS, Christophersen P, Hougaard C *et al*. (2005). Specific enhancement of SK channel activity selectively potentiates the afterhyperpolarizing current IAHP and modulates the firing properties of hippocampal pyramidal neurons. J Biol Chem 280: 41404–41411.

Qi XY, Diness JG, Brundel BJJM, Zhou XB, Naud P, Wu CT *et al*. (2014). Role of small-conductance calcium-activated potassium channels in atrial electrophysiology and fibrillation in the dog. Circulation 129: 430–440.

Schmitt N, Grunnet M, Olesen S-P (2014). Cardiac potassium channel subtypes: new roles in repolarization and arrhythmia. Physiol Rev 94: 609–653.

Singh H, Lu R, Bopassa JC, Meredith AL, Stefani E, Toro L (2013). mitoBKCa is encoded by the Kcnma1 gene, and a splicing sequence defines its mitochondrial location. Proc Natl Acad Sci U S A 110: 10836–10841.

Skibsbye L, Diness JG, Sørensen US, Hansen RS, Grunnet M (2011). The duration of pacing-induced atrial fibrillation is reduced in vivo by inhibition of small conductance Ca(2+)-activated K(+) channels. J Cardiovasc Pharmacol 57: 672–681.

Sørensen US, Strøbæk D, Christophersen P, Hougaard C, Jensen ML, Nielsen E *et al*. (2008). Synthesis and structure-activity relationship studies of 2-(*N*-substituted)-aminobenzimidazoles as potent negative gating modulators of small conductance Ca^{2+}-activated K^+ channels. J Med Chem 51: 7625–7634.

Southan C, Sharman JL, Benson HE, Faccenda E, Pawson AJ, Alexander SPH *et al*. (2016). The IUPHAR/BPS Guide to

PHARMACOLOGY in 2016: towards curated quantitative interactions between 1300 protein targets and 6000 ligands. Nucl Acids Res 44: D1054–D1068.

Stocker M, Pedarzani P (2000). Differential distribution of three Ca(2+)-activated K(+) channel subunits, SK1, SK2, and SK3, in the adult rat central nervous system. Mol Cell Neurosci 15: 476–493.

Strøbæk D, Hougaard C, Johansen TH, Sørensen US, Nielsen EO, Nielsen KS *et al*. (2006). Inhibitory gating modulation of small conductance Ca^{2+}-activated K^+ channels by the synthetic compound (*R*)-*N*-(benzimidazol-2-yl)-1,2,3,4-tetrahydro-1-naphtylamine (NS8593) reduces afterhyperpolarizing current in hippocampal CA1 neurons. Mol Pharmacol 70: 1771–1782.

Strøbæk D, Teuber L, Jørgensen TD, Ahring PK, Kjær K, Hansen RS *et al*. (2004). Activation of human IK and SK Ca^{2+}-activated K^+ channels by NS309 (6,7-dichloro-1*H*-indole-2,3-dione 3-oxime). Biochim Biophys Acta – Biomembr 1665: 1–5.

Waks JW, Zimetbaum P (2017). Antiarrhythmic drug therapy for rhythm control in atrial fibrillation. J Cardiovasc Pharmacol Ther 22: 3–19.

Wulff H, Kolski-Andreaco A, Sankaranarayanan A, Sabatier J-M, Shakkottai V (2007). Modulators of small- and intermediate-conductance calcium-activated potassium channels and their therapeutic indications. Curr Med Chem 14: 1437–1457.

Zoni-Berisso M, Lercari F, Carazza T, Domenicucci S (2014). Epidemiology of atrial fibrillation: European perspective. Clin Epidemiol 6: 213.